Available online at www.sciencedirect.com
ScienceDirect
Chemical Physics Letters xxx (2006) xxx–xxx
CHEMICAL PHYSICS LETTERS
www.elsevier.com/locate/cplett

Theoretical study of intramolecular charge transfer in π-conjugated oligomers

Andrea Amadei [a,*], Marco D'Abramo [b], Alfredo Di Nola [b], Antonio Arcadi [c], Giorgio Cerichelli [c], Massimiliano Aschi [c,*]

[a] *Dipartimento di Scienze e Tecnologie Chimiche Università di Roma, Tor Vergata, via della Ricerca Scientifica 1, I-00133 Roma, Italy*
[b] *Dipartimento di Chimica, Università di Roma, La Sapienza, P.le Aldo Moro 5, 00185 Roma, Italy*
[c] *Dipartimento di Chimica, Ingegneria Chimica e Materiali, Università de l'Aquila, via Vetoio (Coppito 1), 67010 l'Aquila, Italy*

Received 7 November 2006

Abstract

In this Letter, we use the perturbed matrix method, in combination with molecular dynamics and statistical mechanics, in order to describe in details the electric field induced intramolecular charge transfer (ICT) in two π-conjugated oligomers of nanotechnological interest. Results show a relevant relationship between the extent of ICT and molecular conformation, pointing out the highly non-linear charge transfer field response.

1. Introduction

Nature makes use of molecules for promoting many of the basic electronic processes such as photosynthesis and signal transduction. This has stimulated, in the last years, the search for molecular systems aimed at producing electronic devices in the nanoscopic scale [1–7]. In this context, although an impressive number of experimental data has been obtained, much is still obscure at a fundamental level. For instance, not completely clarified is the actual mechanism of molecular conductivity and many related phenomena such as conductance switching [8–12]. In this respect, beyond the successful efforts done by experimentalists, theoretical chemistry may provide the key answers to the above questions, [13–17] and it is common opinion [11] that to understand and predict the properties of such devices it is first necessary to understand the single-molecule physicochemical features. Recently, a systematic theoretical–computational study has been carried out on π-conjugated oligo(phenyleneethynylene) systems (OPE) by Seminario and co-workers [18,19]. These investigations, making use of a joint application of density functional theory (DFT) and Green function formalism, are based on the analysis of usual monoelectronic functions (molecular orbitals) [20]. According to their results a conducting molecular wire is defined as the species which shows frontier orbitals fully delocalized along two metal contacts and, moreover, whose energy is somewhat comparable with the metal Fermi level. This proposed mechanism has been successfully applied for a series of differently substituted OPEs and has represented the first attempt in this direction. More recently, other investigators, using essentially the same computational scheme of Seminario, have underlined the crucial role of internal conformational transitions into the intrinsic properties of OPEs. In this Letter, with the use of perturbed matrix method (PMM), [21,22] we address the same topic but using a different viewpoint, complementary to the one previously described. The basic feature of PMM is the possibility of analyzing the effect of a perturbing electric field on the electronic wavefunction of whatever molecular system at a low computational cost. In fact PMM, based on a quantum-mechanical perturbation procedure,

* Corresponding authors.
E-mail addresses: andrea.amadei@uniroma2.it (A. Amadei), aschi@caspur.it (M. Aschi).

0009-2614/$ - see front matter © 2006 Elsevier B.V. All rights reserved.
doi:10.1016/j.cplett.2006.12.018

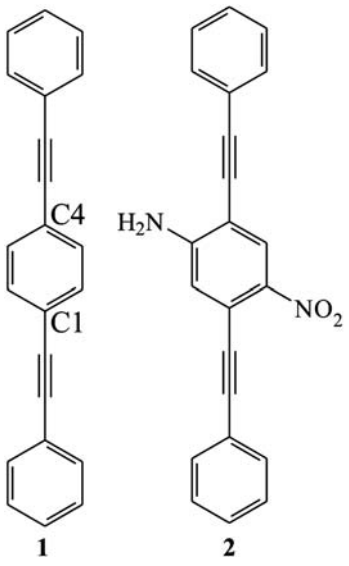

Fig. 1. Schematic view of OPE1 and OPE2.

is able to provide the electronic properties of an atomic-molecular system perturbed by its interaction with the environment, i.e. an external electric field as well as its own conformational transitions. PMM essentially approximates a configuration interaction calculation including the perturbing field in the Hamilton operator. It is worth to note that the previously cited methods, [14,17,18] make use of a single-determinant-based approach applied to a limited (somewhat predefined) set of atomic-molecular conformations. In this Letter, PMM was used to investigate two kinds of OPE, shown in Fig. 1, selected on the basis of their different phenomenological behaviour: one (OPE1) showing a conductive state while the other (OPE2) presenting a conductive state only when reduced [18]. These two molecular systems have been addressed in this Letter as isolated molecules under an external homogenous electric field, in order to pinpoint the effects of the conformational transitions on the intramolecular charge transfer (ICT). In particular, we characterized the molecular field response focussing on the non-linear features of the single molecule charge transfer, which may play a crucial role in the experimentally observed phenomena. We wish to further remark that our aim, in the present study, is the characterization of the possible intrinsic OPE electronic-conformational features and not the detailed reproduction of the experimentally observed process.

2. Theoretical and computational section

Molecular dynamics (MD) simulations were performed for isolated OPE1 and OPE2 without applying any external electric field. The trajectories were propagated for 12.0 ns and the first 2.0 ns were disregarded from the analysis. The temperature was kept at 300 K using the isokinetic temperature coupling [26], constraining the roto-translational motions, [27] for obtaining results fully consistent with statistical mechanics [27] and with the experimental condition where the molecules global motions are constrained by the electrodes. All the bond lengths were constrained using Lincs algorithm [28], and the force fields of the two molecules were constructed as follows: the Lennard-Jones parameters were taken from the Gromos library [24] whereas the atomic point charges were recalculated by means of quantum-chemical calculations in the framework of density functional theory (DFT, see below for details) using standard fitting procedures [29]. A potential energy barrier of 1 kcal/mol was used for modelling [30] the rotation of one ring with respect to the adjacent one. Tests carried out on a spatial grid for the potential energy as provided by the obtained force field with the corresponding potential energy provided by DFT calculations, showed the accuracy of the model employed. GROMACS simulation software package [23,24] implemented in parallel execution, was used for all the simulations.

The trajectories were analyzed using essential dynamics (ED) [25] whose main features are reported elsewhere [25]. Briefly, by diagonalizing all atoms positional fluctuation covariance matrix, as provided by MD simulation, we obtained a set of eigenvectors and eigenvalues. The eigenvectors represent the directions in configurational space and the eigenvalues indicate the mean square fluctuations along these axes. Sorting the eigenvectors by the size of the corresponding eigenvalues, the configurational space can be divided in a low dimensional (essential) subspace in which most of the positional fluctuations are confined and a high dimensional subspace in which merely small vibrations occur. In particular, we characterized the thermodynamics as a function of the position in the essential plane spanned by the first and second eigenvectors. The corresponding free energy surface, i.e. the free energy change for any transition from a reference state to a generic ith state, can be calculated from the corresponding probabilities P_{ref} and P_i respectively (obtained by the MD simulation)

$$\Delta A_i = -kT \ln \frac{P_i}{P_{\text{ref}}} \tag{1}$$

where k is the Boltzmann constant and T the (absolute) temperature. We used a 20×20 grid for defining the conformational states in the essential plane. In this way we obtained a set of eight free energy minima for OPE1 and four free energy minima for OPE2 fully describing all the relevant conformational transitions at 300 K in those molecules. For each minimum we then defined a corresponding free energy basin given by its surrounding region within a free energy variation of 9.0 kJ/mol.

The available experimental data are usually obtained with OPE chemically adsorbed on the electrodes in such a way their molecular roto-translational motions are essentially constrained and, hence, the external field applied has a fixed orientation in the molecular frame (basically parallel to the average OPE principal axis). In order to provide some sort of relationship between our theoretical–compu-

tational results and the information obtained from such an experimental setup, we considered a statistical mechanical ensemble where each OPE molecule, with constrained roto-translational degrees of freedom, may only interact with an electric field parallel to the $C1 \rightarrow C4$ unit vector (see Fig. 1) which corresponds to a completely fixed direction in OPE molecular frame. Moreover, given the weak to moderate field intensity used to reproduce the experimental conditions, we assumed that the free energy basins provided by the MD simulations (not involving the external electric field) still represent all the relevant conformational regions in the presence of the perturbing field.

Therefore for each free energy minimum we extracted a corresponding relaxed molecular structure which was used to provide the basin electronic properties variation due to the field, i.e. we assume the electronic properties of such relaxed structure as representative of the whole basin.

The unperturbed (with no field involved) ground state electronic structure calculations were performed using DFT with PBE0 [31,32] functional in conjunction with the 6-31+G(d) atomic basis set. Ten unperturbed electronic excited states were evaluated by performing time dependent density functional theory (TD-DFT) calculations using the same functional and basis set. The GAUSSIAN 98 [33] package was used at these purposes.

The obtained 11 unperturbed electronic states for each free energy basin, were then used to construct the perturbed (with the field applied as previously described) Hamiltonian matrix to be used in PMM calculations [21].

The resulting perturbed electronic states were used to provide the ICT as a function of the applied field via the variation of the ground state dipole component parallel to the electric field (note that the dipole components orthogonal to the field direction do not undergo any appreciable variation and the use of a field orthogonal to the $C1 \rightarrow C4$ direction does not produce any appreciable charge transfer effect, at least in the field range investigated).

In this way, the ICT induced by the field may be expressed by the corresponding molecular charge variation (Δq) as defined by

$$\Delta q = \frac{\Delta \boldsymbol{\mu} \cdot \boldsymbol{b}}{l} \tag{2}$$

where $\Delta \boldsymbol{\mu}$ is the ground state dipole variation due to the applied field as provided by PMM, $\boldsymbol{b}$ is the $C1 \rightarrow C4$ unit vector defining the field orientation and l is the length of the molecule (ca. 1.9 nm). Note that the thickness of the molecular devices is somewhat larger than 1.9 nm [5], therefore the absolute values of the electric potential (used to report our data) must be considered only as indicative values.

Finally, the unperturbed basin free energies (given by Eq. (1)) and the corresponding perturbed electronic properties (ground state energy and dipole) can be used to obtain the ensemble (thermodynamic) properties related to the actual ICT via basic statistical mechanical relations.

In fact, within the approximation previously described that in each basin the electronic properties variation due to the field is invariant and provided by the corresponding relaxed structure, the canonical partition function of each ith basin (Q_i) may be written as

$$Q_i(E) \cong Q_i(0)\mathrm{e}^{-\beta\Delta\epsilon_i(E)} \tag{3}$$

$$\Delta\epsilon_i(E) = \epsilon_i(E) - \epsilon_i(0) \tag{4}$$

where E is the electric field intensity, ϵ_i is the ground state electronic energy of the relaxed structure in the ith basin and $\beta^{-1} = kT$. From the previous equations we readily obtain the probability P_i and the charge variation expectation value $\langle \Delta q \rangle$

$$P_i(E) = \frac{Q_i(E)}{\sum_l Q_l(E)} \cong \frac{Q_i(0)\mathrm{e}^{-\beta\Delta\epsilon_i(E)}}{\sum_l Q_l(0)\mathrm{e}^{-\beta\Delta\epsilon_l(E)}} = \frac{P_i(0)\mathrm{e}^{-\beta\Delta\epsilon_i(E)}}{\sum_l P_l(0)\mathrm{e}^{-\beta\Delta\epsilon_l(E)}} \tag{5}$$

$$\langle \Delta q \rangle = \sum\nolimits_l P_l(E)\Delta q_l \tag{6}$$

Therefore, the OPE free energy change $\Delta A(E) = A(E) - A(0)$ due to the field in such an ensemble is

$$\Delta A(E) = -kT \ln \frac{\sum_l Q_l(E)}{\sum_l Q_l(0)} \cong -kT \ln \sum\nolimits_l P_l(0)\mathrm{e}^{-\beta\Delta\epsilon_l(E)} \tag{7}$$

3. Results and discussion

As described in the previous section, the analysis of the free energy surface on the essential plane provided eight and four free energy basins for OPE1 and OPE2, respectively, whose relative unperturbed free energies are reported in Table 1 and Table 2. In the same tables, we also report the main geometrical parameters characterizing the free energy minima relaxed structures (schematically shown in Fig. 2), utilized to obtain the electronic properties of each basin as reported in the previous section. It is worth to note that the two essential eigenvectors defining the essential plane, i.e. providing the conformational transitions among the free energy basins, mainly correspond in both molecules to a concerted $\phi 1$ and $\phi 2$ rotation (first eigenvector), and to the bending τ mode (second eigenvector).

Table 1
Unperturbed Helmholtz free energy differences, $\phi 1$, $\phi 2$ and τ (see text and Fig. 1) of the eight basins of OPE1 at 300 K

Basin	ΔA (kJ/mole)	$\phi 1$(°)	$\phi 2$(°)	τ(°)
1a	6.0	0	0	180
1b	5.0	−79	−60	175
1c	0.0	−20	20	176
1d	6.0	24	−20	164
1e	0.2	−8	0	172
1f	0.3	−40	20	179
1g	5.0	−80	−81	175
1h	0.3	−19	1	175

The dihedral angles ($\phi 1$ and $\phi 2$) provide the rotation of ring1 and ring3, respectively, with respect to the central one. Finally, the angle τ is defined by the geometrical centres of the three rings.

Please cite this article in press as: A. Amadei et al., Chem. Phys. Lett. (2006), doi:10.1016/j.cplett.2006.12.018

Table 2
Unperturbed Helmholtz free energy differences, $\phi 1$, $\phi 2$ and τ (see text and Fig. 1) of the four basins of OPE2 at 300 K

Basin	ΔA (kJ/mole)	$\phi 1(^\circ)$	$\phi 2(^\circ)$	$\tau(^\circ)$
2a	0.0	0.0	0.0	180
2b	3.0	−25	−20	175
2c	3.0	12	18	172
2d	2.0	−76	100	176

The dihedral angles ($\phi 1$ and $\phi 2$) provide the rotation of ring1 and ring3, respectively, with respect to the central one. Finally, the angle τ is defined by the geometrical centres of the three rings.

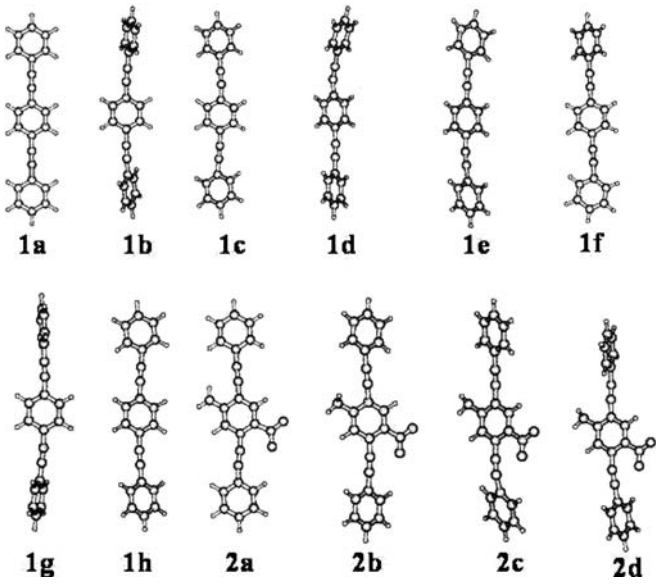

Fig. 2. Free energy minima relaxed structures, representative of the basins, as obtained by MD simulation at 300 K for the unperturbed OPE1 and OPE2.

It is interesting to observe that the basin characterized by a fully planar carbon framework (**1a** and **2a** for OPE1 and OPE2, respectively), the stable structure at 0 K, only in OPE2 corresponds to the absolute free energy minimum at 300 K in the absence of the electric field. This is due to the presence of the $-NH_2$ and $-NO_2$ substituents stabilizing, via electrostatic effects, the fully planar configuration.

In Fig. 3, we compare the ICT of OPE1 and OPE2, expressed by the charge separation expectation value, as obtained by PMM/MD using Eqs. (5) and (6). Note that such a property is obtained considering the whole conformational ensemble and therefore includes both the field effect on each free energy basin electronic behaviour as well as on the relative basin stability. Note that the curves in the figure are not necessarily to be symmetric (they would be somewhat symmetric only at 0 K) as indeed observed at relatively high voltage. From the figure, it is evident the rather different electric field response of OPE1 and OPE2 in line with the available experimental data [34]. Interestingly OPE1 presents two significant switches, one at about ±6 V and the other at about ±9 V, providing the observed higher ICT of OPE1 compared to OPE2.

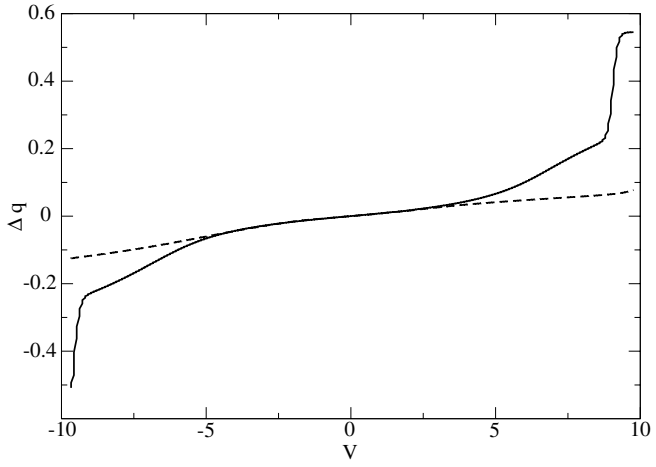

Fig. 3. Intramolecular charge transfer of OPE1 (solid) and OPE2 (dashed) molecules. The perturbing homogeneous field applied is expressed via the corresponding electric potential difference for ca 2 nm distance, i.e. the molecular length.

In order to identify the physical nature of the observed OPE1 behavior, we analyzed the ICT features of each free energy basin showing essentially two different behaviors reported in Fig. 4. The dashed curve, providing the ICT of the basins characterized by roughly coplanar rings (**1a**, **1c**, **1d**, **1e**, **1f** and **1h**), is clearly responsible of the first OPE1 switch at about ±6 V, while the solid curve showing the charge transfer behavior of the **1b** and **1g** basins, characterized by the external rings roughly orthogonal to the central one, clearly provides the dramatic OPE1 switch at about ±9 V. Therefore, the OPE1 ICT as shown in Fig. 3, is determined by the probability balance of these two basin groups which present a rather different charge transfer response to the perturbing electric field. Interestingly the weak OPE2 ICT in the electric field range investigated (Fig. 3), can be

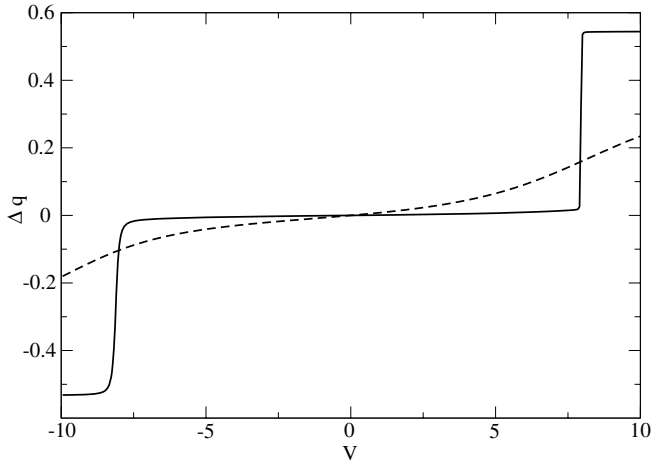

Fig. 4. Intramolecular charge transfer of **1d** (dashed) and **1g** (solid) basin structures representative of the {**1a**, **1c**, **1d**, **1e**, **1f**, **1h**} and {**1b**, **1g**} basin groups, respectively. The perturbing homogeneous field applied is expressed via the corresponding electric potential difference for ca 2 nm distance, i.e. the molecular length.

Please cite this article in press as: A. Amadei et al., Chem. Phys. Lett. (2006), doi:10.1016/j.cplett.2006.12.018

ascribed not only to the weaker response of each basin but also to the absence of the dramatic switch observed in OPE1 **1b** and **1g** basins. Remarkably OPE2 **2d** basin, characterized by a structural organization similar to **1b** and **1g**, provides a dramatic switch resembling the **1b** and **1g** ones, at higher perturbing field (about 12.0 V) pointing out the striking relationship between molecular structure and conductivity already considered by other authors [8,20,17].

In Fig. 5, we report the probability for the two OPE1 basin groups, i.e. {**1a**, **1c**, **1d**, **1e**, **1f**, **1h**} and {**1b**, **1g**}, as a function of the perturbing field as provided by Eq. (5). The figure clearly shows that up to about ±5 V the **1b** and **1g** basins are thermodynamically rather unstable becoming, by far, the most stable basins at higher field and hence ruling the conductivity/conformational behavior of the molecule in the highest field range considered.

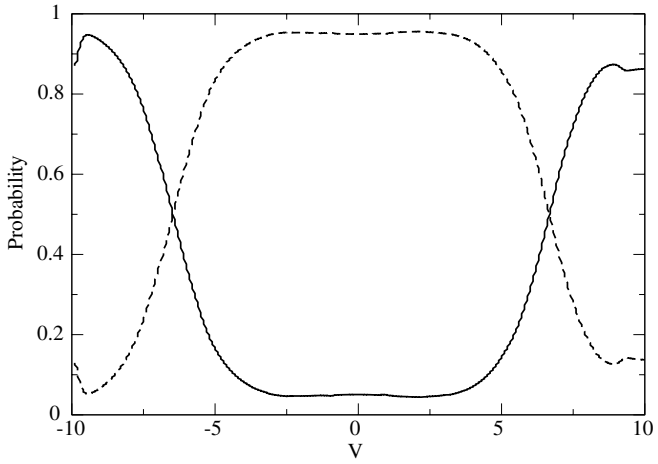

Fig. 5. Probability of the two OPE1 basin groups. {**1a**, **1c**, **1d**, **1e**, **1f**, **1h**} dashed line; {**1b**, **1g**} solid line. The perturbing homogeneous field applied is expressed via the corresponding electric potential difference for a 2 nm distance, i.e. the molecular length.

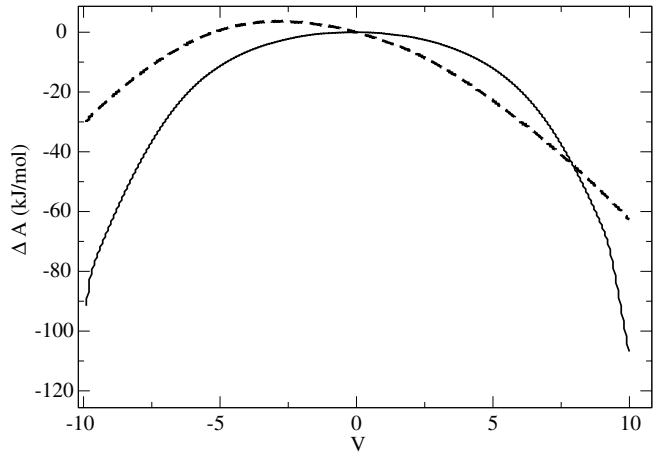

Fig. 6. Free energy variation due to the applied field for OPE1 (solid) and OPE2 (dashed) molecules. The perturbing homogeneous field applied is expressed via the corresponding electric potential difference for ca 2 nm distance, i.e. the molecular length.

Finally, we evaluated the field effect on the thermodynamic stability of OPE1 and OPE2 molecules in terms of the free energy change due to the electric field Eq. (7), as reported in Fig. 6. The figure shows the OPE1 higher stability in the high field range reflecting the OPE1 higher ICT and the presence of the dramatic charge transfer switch at about ±9 V. Interestingly in both molecules the free energy curve is not fully symmetric as a consequence of the conformational equilibria involving asymmetric structures with hence a not fully symmetric field response.

4. Conclusions

The theoretical–computational investigation described in this Letter has demonstrated a relevant structure-conductivity relationship in π-conjugated oligomers, remarkably pointing out the presence of conformers with a highly non-linear charge transfer field response. Given the multiple conformational states accessible at functional conditions in these molecules, such a feature implies that the observed intramolecular charge transfer are largely affected by the conformational equilibria determined by the proper statistical mechanical ensemble of the molecule. Such results, in line with previous [17] computational studies, indicate the complexity of the intramolecular charge transfer which involves both single structure conductivity as well as conformational transitions implying that, even for isolated molecules, a statistical mechanical approach is mandatory in order to provide reliable results to be compared to experimental data.

Finally, this investigation confirms the ability of the combined PMM/MD procedure to provide a rather complete and accurate statistical mechanical model for the physical-chemical behavior including the electronic properties.

Acknowledgements

We acknowledge University of L'Aquila for financial support.

References

[1] J.M. Tour, Molecular Electronics: Commercial Insights, Chemistry, Devices, Architecture and Programming, World Scientific Publishing, River Edge, NY, 2003.
[2] M.D. Ward, J. Chem. Educ. 78 (2001) 321.
[3] J.R. Heath, Pure Appl. Chem. 72 (2000) 11.
[4] R. Overton, Wired 8 (2000) 242.
[5] D.K. James, J.M. Tour, Anal. Chim. Acta 568 (2006) 2.
[6] J.M. Tour, Acc. Chem. Res. 33 (2000) 791.
[7] D.K. James, J.M. Tour, Aldrichim. Acta 39 (2006) 47.
[8] J. Cornil, Y. Karzazi, J. Bredas, J. Am. Chem. Soc. 124 (2002) 3516.
[9] F.-R.F. Fan et al., J. Am. Chem. Soc. 124 (2002) 5550.
[10] Z.K. Keane, J.W. Ciszek, J.M. Tour, D. Natelson, Nano Lett. 6 (2006) 1518.
[11] P.A. Lewis, C.E. Inman, F. Maya, J.M. Tour, J.E. Hutchison, P.S. Weiss, J. Am. Chem. Soc. 127 (2005) 17421.
[12] A.M. Moore et al., J. Am. Chem. Soc. 128 (2006) 1959.

[13] N.D. Lang, P. Avouris, Phys. Rev. B 62 (2000) 7325.
[14] C.W. Baushlicher, A. Ricca, N. Mingo, J. Lawson, Chem. Phys. Lett. 372 (2003) 723.
[15] J.M. Seminario, A.G. Zacarias, J.M. Tour, J. Am. Chem. Soc. 120 (1998) 3970.
[16] E.G. Emberly, G. Kirczenow, Phys. Rev. B 64 (2001) 235412.
[17] J. Taylor, M. Brandbyge, K. Stokbro, Phys. Rev. B 68 (2003) 121101.
[18] J.M. Seminario, A.G. Zacarias, P.A. Derosa, J. Phys. Chem. A 105 (2001) 791.
[19] J.M. Seminario, A.G. Zacarias, P.A. Derosa, J. Chem. Phys. 116 (2002) 1671.
[20] P.A. Derosa, S. Guda, J.M. Seminario, J. Am. Chem. Soc. 125 (2003) 14240.
[21] M. Aschi, R. Spezia, A. Di Nola, A. Amadei, Chem. Phys. Lett. 344 (2001) 374.
[22] A. Amadei, F. Marinelli, M. D'Abramo, M. D'Alessandro, M. Anselmi, A. Di Nola, M. Aschi, J. Chem. Phys 122 (2005) 124506.
[23] D. van der Spoel et al., Gromacs User Manual Version 1.3, 1996. <http://rugmd0.chem.rug.nl/gmx>.
[24] W.F. van Gunsteren et al., Biomolecular Simulation: The GROMOS96 Manual and User Guide, Hochschulverlag AG an der ETH Zürich, Zürich, 1996.
[25] A. Amadei, A.B.M. Linssen, H.J.C. Berendsen, Proteins: Struct. Funct. Gen. 17 (1993) 412.
[26] D.J. Evans, G.P. Morriss, Statistical Mechanics of Nonequilibrium Liquids, Academic Press, London, 1990.
[27] A. Amadei, G. Chillemi, M.A. Ceruso, A. Grottesi, A. Di Nola, J. Chem. Phys. 112 (2000) 9.
[28] B. Hess, H. Bekker, H.J.C. Berendsen, J.G.E.M. Fraaije, J. Comput. Chem. 18 (1997) 1463.
[29] C.I. Bayly, P. Cieplak, W.D. Cornell, P.A. Kollman, J. Phys. Chem. 97 (1993) 10269.
[30] J.M. Seminario, P.A. Derosa, J.L. Bastos, J. Am. Chem. Soc. 124 (2002) 10266.
[31] J.P. Perdew, Y. Wang, Phys. Rev. B 45 (1992) 13244.
[32] J.P. Perdew, K. Burke, M. Ernzerhof, Phys. Rev. Lett. 77 (1996) 3865.
[33] Gaussian 98 Revision A.7, Gaussian, Inc., Pittsburgh, PA, 1998.
[34] J. Chen, W. Wang, M.A. Reed, Appl. Phys. Lett. 77 (2000) 1224.

Please cite this article in press as: A. Amadei et al., Chem. Phys. Lett. (2006), doi:10.1016/j.cplett.2006.12.018